

Isomerization of an Azobenzene Derivative on a Thin Insulating Layer by Inelastically Tunneling Electrons

Ali Safiei, Jörg Henzl, and Karina Morgenstern*

Institut für Festkörperphysik, Abteilung ATMOS, Leibniz Universität Hannover, Appelstrasse 2, D-30167 Hannover, Germany

(Received 12 February 2010; published 25 May 2010)

Scanning tunneling microscopy is used to investigate isomerization of amino-nitro-azobenzene on a thin NaCl layer on Ag(111) by inelastically tunneling electrons. A reversible isomerization between a planar *trans* and a three-dimensional *cis* form with two different thresholds is demonstrated. The isomerization characteristics are rationalized in terms of binding of the multipolar molecule to the ionic layer. This study shows the feasibility of a bistable single molecule switch on an insulator.

DOI: 10.1103/PhysRevLett.104.216102

PACS numbers: 68.37.Ef, 68.43.Hn, 68.65.-k, 82.37.Gk

The emerging field of molecular electronics needs a possibility to interconvert energy, e.g., electric into mechanical energy. Dye molecules are attractive for such molecular switches [1,2]. Amongst these, azobenzene derivatives ($C_6H_5N=NC_6H_5$), studied extensively in solution and the fluid-crystalline phase [3–6], make a light-induced transition between an extended (*trans*) and a compact (*cis*) configuration. As integration of molecules into circuits demands an arrangement on surfaces, the feasibility of switching single molecules on metallic surfaces was demonstrated by scanning tunneling microscopy (STM) [7–12]. However, circuits are rather placed on insulators in order to reduce stray currents.

Thin NaCl layers are model systems for insulators. They allow to investigate the functionalities of molecules with lower coupling to the substrate than a metal surface. This was successfully demonstrated for tautomerization of naphthalocyanine [13] and for charging of single adatoms [14,15]. This decoupling allows to directly image molecular orbitals [16].

Dye molecules have not yet been investigated on insulating supports. We shortly review work for azobenzene (AB) on Au(111), the least interacting surface studied so far. Isomerization lifts one side of the molecule from the surface for native [8] and poly-*tert*-butyl-AB [9], while amino-nitro-AB switches between two planar configurations [7,10]. The importance of the end groups was further underlined by the study of 4-dimethylamino-AB-4'-sulfonic acid, for which isomerization is not reversible [11]. Mostly, isomerization was induced by inelastically tunneling electrons (IET), but within islands the isomerization of poly-*tert*-butyl-AB was induced by the electric field [9], by light [12,17,18], or thermally [19].

Here, we investigate *cis-trans* isomerization of amino-nitro-azobenzene on a thin NaCl layer on Ag(111) by STM. A reversible switching with two different thresholds is demonstrated. It is shown that the behavior of this switch on an insulator can not be predicted from its properties on metals and that the atomic scale details of insulators have to be considered for small molecules.

The experiments were performed with a low-temperature STM. The STM is housed in a UHV chamber with standard facilities for sample cleaning. The base pressure is 8×10^{-10} mbar, the pressure during adsorption is reduced to 4×10^{-10} mbar by a cold trap. The single crystalline Ag(111) surface is cleaned by cycles of Ne^+ sputtering and annealing. NaCl islands of approximately 20 nm side length are grown close to room temperature by evaporation with a rate of 0.02 ML/min. On Ag(111) as on similar surfaces (e.g., Cu(111) [20]) the NaCl grows in double layers. Amino-nitro AB [Fig. 1(a)] is deposited from a Knudsen cell onto the sample held at 17 K. Measurements are performed at 5 K.

IET manipulation is performed by positioning the tip above the center of the molecule, freezing the tip-sample distance, and increasing current and voltage to predefined values given in the figure captions. The current is recorded during the manipulation and sharp changes are indicative of the success of the manipulation. This is confirmed by a STM image taken afterwards.

We start by characterizing the molecule adsorbed on the NaCl islands. After adsorption additional protrusions are observed some of them in pairs [Fig. 1(b)]. The pairs of protrusions are reminiscent of the *trans* isomer adsorbed on Au(111) [7,8]. Amino-nitro-AB consisted of two protrusions with a distance of 1.05 nm and an apparent height of 100 pm. Here, a distance of (1.03 ± 0.12) nm between the mean of two Gaussian fits to the line scan with an apparent height of (47 ± 10) pm is measured in the voltage range of 120 to 380 mV. Apparent heights and lateral distances should in general depend on the tip structure. However, those tips that allow to image the molecules without moving them or even the NaCl islands show very little variation in height of the order of 5 to 10 pm. Position of the maxima vary by ± 0.1 nm.

The STM image is not consistent with imaging the lowest unoccupied molecular orbital (LUMO) or highest occupied molecular orbital (HOMO) or a combination of the two orbitals [Fig. 1(f)]. It could be explained by the superposition of more orbitals broadened into the gap, e.g.,

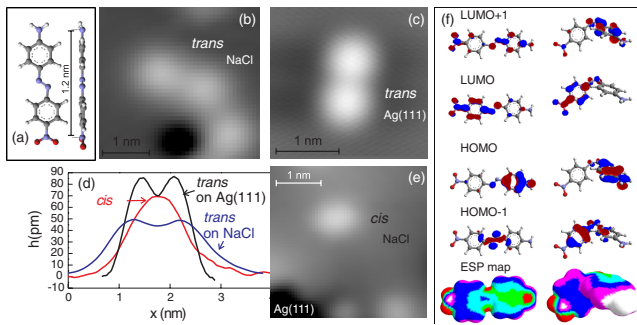


FIG. 1 (color online). Amino-nitro-AB adsorbed at 17 K on Ag(111): (a) top view and side view of the *trans* isomer as optimized in the gas phase with ArgusLab 4.0 [28] (b) *trans* isomer on a NaCl double layer, 30 pA, 376 mV; two protrusions have an apparent height of (46 ± 12) pm and a distance of (1.07 ± 0.12) nm as determined in a statistical analysis (c) *trans* isomer on Ag(111), 57 pA, 158 mV; (d) line scans across molecules as indicated (e) *cis* isomer on a NaCl double layer, 28 pA, 0.12 V (f) orbitals of molecule and ESP map in gas phase as calculated by ArgusLab 4.0 [28]; note that the LUMO + 1 and HOMO - 1 correspond to the HOMO and LUMO of the native azobenzene; in the ESP map the red, yellow, and green regions are with decreasing weight those with most negative density and should thus dominate a STM image [21].

the four orbitals shown in Fig. 1(f). Contribution from multiple orbitals is captured in the ESP (electrostatic potential) map concept for physisorbed molecules [21], from which most intensity is expected at the nitro and the amino group and some further intensity from the azo group [Fig. 1(f)] consistent with the observed image.

The molecule on Ag(111) exhibits a larger height of 85 pm, but a distance between the protrusions of 0.7 nm only [Fig. 1(c) and 1(d)]. The latter distance is rather consistent with the phenyl rings being imaged than the end groups, while the larger distance on NaCl is closer to the distance of the nitrogen atoms of the end groups in the gas phase of 1.2 nm [Fig. 1(a)]. Decreasing interaction with the surface thus leads to a shift of the highest conductivity from the aromatic ring to the end groups consistent with a physisorbed molecule [21]. Thus, the NaCl layer indeed decouples the molecule from the metallic substrate.

The molecules are thereby adsorbed at two different angles of $(19^\circ \pm 5^\circ)$ and of $(41^\circ \pm 3^\circ)$ with respect to the (001) oriented NaCl lattice (cf. Fig. 4 below). These adsorption rotamers can be interconverted by IET manipulation as demonstrated in Fig. 2.

We have thus identified a pair of protrusions with a distance of slightly above 1 nm as intact molecules [Fig. 1(b)]. This identification is corroborated by the manipulation experiments.

We now manipulate the *trans*-isomer by injecting electrons into the azo group (Fig. 3). This manipulation leads to an ellipsoidal protrusion [Fig. 3(b)]. Figure 1(e) shows a high-resolution image of the manipulated species. The line scan in Fig. 1(d) compares it to the original molecule. The protrusion after manipulation is slightly asymmetric and its

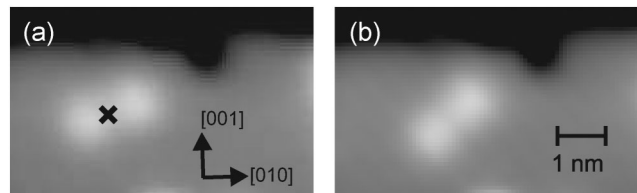


FIG. 2. Snapshots of a series of IET manipulations of *trans*-amino-nitro-AB between two adsorption configurations, manipulation with 660 mV, 40 pA, 1.4 s, imaging parameters: 30 pA, 376 mV.

apparent height above the NaCl is larger than the one of the *trans* isomer. An ellipsoidal protrusion was interpreted before as a *cis*-molecule with only one of the phenyls staying planar to the surface, while the other one turns out-of-plane [8] (see ball-and-stick models in Fig. 3). Such an out-of-plane isomer reflects the gas phase *cis* isomer, in which the phenyls are also turned out of the N = N plane because of steric repulsion. The ellipsoidal protrusion thus represents the *cis* isomer. The series in Fig. 3 demonstrates the reversibility and bistability of switching between the two isomers.

As a corollary, we remark that around 23% of the single protrusions found after adsorption exhibit the apparent height of the *cis* isomer. Thus, the adsorption itself converts the gas phase *trans* to the *cis* isomer. The adsorption energy is thus sufficient to overcome the isomerization threshold [22].

We now discuss the energetic thresholds of the isomerization. Below 600 mV no isomerization is observed on the experimental time scale. The *trans* to *cis* isomerization is possible between 600 and 650 mV with a low yield of $1.5 \times 10^{-9}/e^-$. A threshold at (650 ± 10) mV leads to a

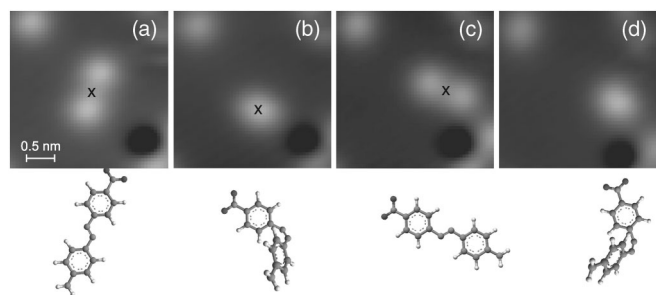


FIG. 3. Reversible isomerization of single amino-nitro-AB molecule: ball-and-stick models in the same orientation but not to scale, $I = 30$ pA, $V = 0.76$ V: (a) before injection of electrons with 640 mV, 50 pA for 700 ms, where indicated by cross (b) after first injection and before injection of electrons with 700 mV, 50 pA for 700 ms (c) after second injection and before injection of electrons with an energy of up to 640 mV, 50 pA for 700 ms (d) after third injection; the single protrusion and single depression on the image remain unaltered serving as a marker and visualize IET induced diffusion of the manipulated molecule.

substantial increase in yield to $2.4 \times 10^{-8}/e^-$. For the *cis* isomer, no isomerization but instead diffusion is induced at 680 meV and below. At 700 meV and above isomerization is possible as demonstrated by the series in Fig. 3. In all cases diffusion or even desorption is induced after the isomerization. Though the yield for *cis-trans* isomerization is with $\approx 3.6 \times 10^{-8}/e^-$ at 700 mV larger than the *trans-cis* isomerization, the yield for diffusion below threshold is even larger, being already $\approx 5.5 \times 10^{-8}/e^-$ at 640 mV. This points towards a smaller binding energy of the *cis* isomer as compared to the *trans* isomer. Diffusion is thereby rather an additional reaction than a concurrence reaction to isomerization. Suppression of diffusion by anchoring of a related molecule within supramolecular assemblies suppresses diffusion completely but does not change the isomerization yield substantially [23].

Comparison of the energetic threshold to the electronic structure of AB molecules adsorbed on metal surfaces shows that the orbitals usually involved in photoisomerization with large weight at the azo group, here HOMO - 1 and LUMO + 1 [Fig. 1(f)] cannot be responsible for the isomerization. Those orbitals have been measured for different azobenzene derivatives on Au(111) and Ag(111) by photoemission and by scanning tunneling spectroscopy beyond 1 eV in all cases [8,18,23,24]. The end groups here induce two additional orbitals [Fig. 1(f), HOMO and LUMO] that might be accessible, but have only little weight at the azo group. We might thus consider a scenario, in which the molecule is electronically excited via one of these orbitals and then the energy is distributed into vibrational modes that eventually lead to isomerization. However, two observations contradict this interpretation: (i) The threshold of *trans-cis* isomerization is symmetric with respect to the Fermi energy; the calculated gap is however 3.1 and 3.2 eV for *cis* and *trans* isomer, respectively [25]. (ii) The STM image is invariant also in the range of and slightly above the threshold. If the LUMO was situated at the threshold, we would expect the STM image to change substantially [16]. Alternatively, molecular vibrations might be excited directly [26]. As the excitation energy thresholds is too high for a singly excited vibration, the threshold rather corresponds to the energetic barrier between the two isomers. In this case, a higher energy for the *cis* to *trans* than for the *trans* to *cis* isomerization points to an asymmetric potential energy surface, which is inversed with respect to the potential energy surface in the gas phase. Thereby, the *cis* isomer is ≈ 100 meV more stable than the *trans* isomer.

We now discuss the results presented above with respect to isomerization of the same molecule on Au(111) [7]. The yield is $\approx 7 \times 10^{-8}$ on Au(111) and thus larger than both isomerization yields on NaCl. This is not expected, because decoupling of the molecule from the metal supposedly quenches alternative deexcitation channels, e.g., via electron-hole pair formation. Another important difference is the dimensionality of the *cis*-isomer that is three-dimensional on the NaCl layer, but two-dimensional on

Au(111), where both phenyls stay planar to the surface. Despite this major difference, the threshold for *trans-cis* isomerization is 650 meV in both cases. In contrast, the threshold for *cis-trans* isomerization on Au(111) was smaller than 640 meV and here on NaCl it is 700 meV. Thus the stability of the *cis* isomers is reversed on the two surfaces. Though it is not surprising that the isomer that more resembles the gas phase is more stable than the one strained into two dimensionality, it is surprising that the *cis* isomer is more stable than the *trans* isomer at all. In the gas phase the *trans* isomer is always the more stable one.

We explain this at first sight unexpected behavior based on high-resolution images with a functionalized tip [Fig. 4(a)]. While atomic resolution is not possible with a “regular” tip without altering the position of the molecules, a functionalized tip allows to image the chlorine lattice [27] and the position of the molecules simultaneously. Determination of their adsorption site from such an image is possible without further molecular resolution because of the molecule’s symmetry.

Figure 4(b) shows the two adsorption rotamers of the *trans* isomer. The adsorption sites reveal the difficulty of the molecule to accommodate to the ionic support. A highly electronegative group (NO_2) will always try to align close to cations and the electropositive group (NH_2) will align to anions. However, the common motif of both molecules shown is the adsorption site of the azo group, which thus steers the adsorption. This result is corroborated by adsorption experiments of an AB with different end groups (*p*-hydroxy-AB, not shown). The double bond prefers to reside above a fourfold hollow site, in between two anions and two cations. The orientation of molecule A puts the nitro group near a cation. This, however, forces the amino group close to a similar adsorption site, which is energetically not favorable (or vice versa for interchanged end groups). The orientation of molecule B brings the amino group energetically favorable near an anion, but it forces the nitro group close to a similar, but energetically unfavorable, adsorption site. Note that the complete adsorption energetics involves not only electrostatics, but also interaction via the aromatic rings. However, this quali-

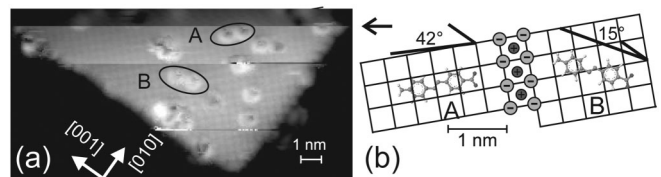


FIG. 4. Adsorption site determination: (a) STM image with functionalized tip, 33 pA, 120 mV; tip picks up molecular part at arrow leading to atomic resolution in the lower part of the image; two molecules A and B are marked with ellipses (b) grid of chlorine atoms around molecules A and B as extracted from (a); ionic lattice is indicated by balls; angle denotes direction of molecule with respect to the nonpolar step edges of the NaCl islands; end groups of amino-nitro-AB may be interchanged, because they do not differ in the images.

tative discussion demonstrates the general difficulty of the *trans* isomer to adapt a favorable adsorption site.

Based on this observation, we rationalize the experimental findings. The *cis* molecule is more stable than the *trans* molecule, because for the latter only two of the three interacting groups can be accommodated with an energy gain. Thus bringing the third group back to the surface is energetically unfavorable.

Finally, we comment on the reduced yield. For this, it should be kept in mind, that the measured yield contains three steps: First, not all electrons that flow from the tip to the sample interact with the molecule. This is reflected in the apparent height of molecules that largely underestimates their real in STM images. Then, from these tunneling electrons only a small percentage interacts inelastically and excites the molecule. Finally, only some of the excited molecules will isomerize, while the others deexcite through alternative deexcitation channels, e.g., electron-hole pair excitation on metals. It is only the latter step that should be increased upon decoupling the molecule from the metal. In contrast the first yield is decreased on the insulating layer as deduced from the reduced apparent height, which persists up to 760 meV [Fig. 1(d)]. Under the assumption of a comparable percentage of the second step, the yield of the excited molecules that isomerize is of the same order of magnitude contrary to expectation. To understand this phenomenon excited-state calculations of the molecules would be necessary, which are not yet feasible for such a large molecule.

In conclusion, we demonstrated the feasibility of isomerization of a single dye molecule on an ultrathin insulating layer. The molecules can be switched in a controlled fashion between the two states by excitation through inelastic tunneling electrons. The isomerization characteristics is rationalized in terms of binding of the multipolar molecule to the ionic layer. This hitherto unexplored field of isomerization on insulating layers is a further step towards the realization of molecular electronics. The bistability of the molecules makes them ideal candidates for molecular switches. Different end groups should be explored for designing an isoenergetic bistability. It can be anticipated that the diffusion can be reduced by embedding the switchable unit into larger molecules with defined anchoring groups.

We acknowledge financial support from the Deutsche Forschungsgemeinschaft.

* morgenstern@fkp.uni-hannover.de

- [1] T. Ikeda and O. Tsutsumi, *Science* **268**, 1873 (1995).
- [2] N. Tamai and H. Miyasaka, *Chem. Rev.* **100**, 1875 (2000).
- [3] S. Monti, G. Orlandi, and P. Palmieri, *Chem. Phys.* **71**, 87 (1982).
- [4] T. Nägele, R. Hoche, W. Zinth, and J. Wachtveitl, *Chem. Phys. Lett.* **272**, 489 (1997).

- [5] *Molecular Switches*, edited by B. L. Feringa (Wiley-VCH, Weinheim, 2001).
- [6] T. Ishikawa, T. Noro, and T. Shoda, *J. Chem. Phys.* **115**, 7503 (2001).
- [7] J. Henzl, M. Mehlhorn, H. Gawronski, K.-H. Rieder, and K. Morgenstern, *Angew. Chem., Int. Ed.* **45**, 603 (2006).
- [8] B. Y. Choi, S. J. Kahng, S. Kim, H. Kim, H. W. Kim, Y. J. Song, J. Ihm, and Y. Kuk, *Phys. Rev. Lett.* **96**, 156106 (2006).
- [9] M. Alemani, M. V. Peters, S. Hecht, K.-H. Rieder, F. Moresco, and L. Grill, *J. Am. Chem. Soc.* **128**, 14446 (2006).
- [10] J. Henzl, M. Mehlhorn, and K. Morgenstern, *Nanotechnology* **18**, 495502 (2007).
- [11] J. Henzl, Th. Bredow, and K. Morgenstern, *Chem. Phys. Lett.* **435**, 278 (2007).
- [12] M. J. Comstock, N. Levy, A. Kirakosian, J. Cho, F. Lauterwasser, J. H. Harvey, D. A. Strubbe, J. M. J. Frechet, D. Trauner, S. G. Louie, and M. F. Crommie, *Phys. Rev. Lett.* **99**, 038301 (2007).
- [13] P. Liljeroth, J. Repp, and G. Meyer, *Science* **317**, 1203 (2007).
- [14] J. Repp, G. Meyer, F. E. Olsson, and M. Persson, *Science* **305**, 493 (2004).
- [15] F. E. Olsson, S. Paavilainen, M. Persson, J. Repp, and G. Meyer, *Phys. Rev. Lett.* **98**, 176803 (2007).
- [16] C. J. Villagomez, T. Zambelli, S. Gauthier, A. Gourdon, C. Barthes, S. Stojkovic, and Ch. Joachim, *Chem. Phys. Lett.* **450**, 107 (2007).
- [17] S. Hagen, F. Leyssner, D. Nandi, M. Wolf, and P. Tegeder, *Chem. Phys. Lett.* **444**, 85 (2007).
- [18] S. Hagen, P. Kate, F. Leyssner, D. Nandi, M. Wolf, and P. Tegeder, *J. Chem. Phys.* **129**, 164102 (2008).
- [19] L. Ovari, M. Wolf, and P. Tegeder, *J. Phys. Chem. C* **111**, 15370 (2007).
- [20] J. Repp, G. Meyer, and K.-H. Rieder, *Phys. Rev. Lett.* **92**, 036803 (2004).
- [21] H. Gawronski, J. Henzl, V. Simic-Milosevic, and K. Morgenstern, *Appl. Surf. Sci.* **253**, 9047 (2007).
- [22] Some of the molecules dissociate during adsorption. Those molecules that remain intact are not dissociated by IET manipulation in the voltage range of isomerization.
- [23] J. Henzl and K. Morgenstern, *Phys. Chem. Chem. Phys.*, doi:10.1039/b924488c (2010).
- [24] P. Tegeder, S. Hagen, F. Leyssner, M. V. Peters, S. Hecht, T. Klamroth, P. Saalfrank, and M. Wolf, *Appl. Phys. A* **88**, 465 (2007).
- [25] G. Fücksel, T. Klamroth, J. Dokic, and P. Saalfrank, *J. Phys. Chem. B* **110**, 16337 (2006); G. Fücksel (private communication).
- [26] W. Ho, *J. Chem. Phys.* **117**, 11033 (2002).
- [27] W. Hebenstreit, J. Redinger, Z. Horozora, M. Schmid, R. Podlocky, and P. Varga, *Surf. Sci.* **424**, L321 (1999).
- [28] M. A. Thomson, Planaria Software, LCC, Seattle, WA, www.arguslab.com using the semiempirical Austin Model 1 methods for the quantum calculation of the molecular electronic structure; for details see M. J. S. Dewar, E. G. Zoebisch, E. F. Healy, and J. J. P. Stewart, *J. Am. Chem. Soc.* **107**, 3902 (1985).